Ultrafast time-resolved spectroscopy elucidating photo-driven electron and energy transfer processes in a broadband light-absorbing BODIPY-C60-distyryl BODIPY triad

Anam Fatima, Jad Rabah, Emmanuel Allard, Hélène Fensterbank, Karen Wright, Gotard Burdzinski, Fabien Miomandre, Julie Pham, Gilles Clavier, Michel Sliwa, et al.

Eur. Phys. J. Special Topics (2022)

https://doi.org/ 10.1140/xxxxx (will be inserted by the publisher)

Ultrafast time-resolved spectroscopy elucidating photo-driven electron and energy transfer processes in a broadband light-absorbing BODIPY-C_{60}-distyryl BODIPY triad

A. Fatima,[1] J. Rabah,[2] E. Allard,[2] H. Fensterbank,[2] K. Wright,[2] G. Burdzinski,[3] F. Miomandre,[4] J. Pham,[4] G. Clavier,[4] M. Sliwa,[5] T. Pino,[1] R. Méallet-Renault,[1]* K. Steenkeste,[1]* M. H. Ha-Thi[1]**

[1] Université Paris-Saclay, CNRS, Institut des Sciences Moléculaires d'Orsay, 91405, Orsay, France

[2] Université Paris-Saclay, UVSQ, CNRS, Institut Lavoisier de Versailles, 78000, Versailles, France.

[3] Adam Mickiewicz Univ in Poznan, Fac Phys, Quantum Elec. Lab, PL-61614 Poznan, Poland

[4] Université Paris-Saclay, ENS Paris-Saclay, CNRS, PPSM, 91190 Gif-sur-Yvette, France

[5] Univ. Lille, CNRS, UMR 8516, LASIRE, Laboratoire de Spectroscopie pour les Interactions, la Réactivité et l'Environnement, F59 000 Lille, France

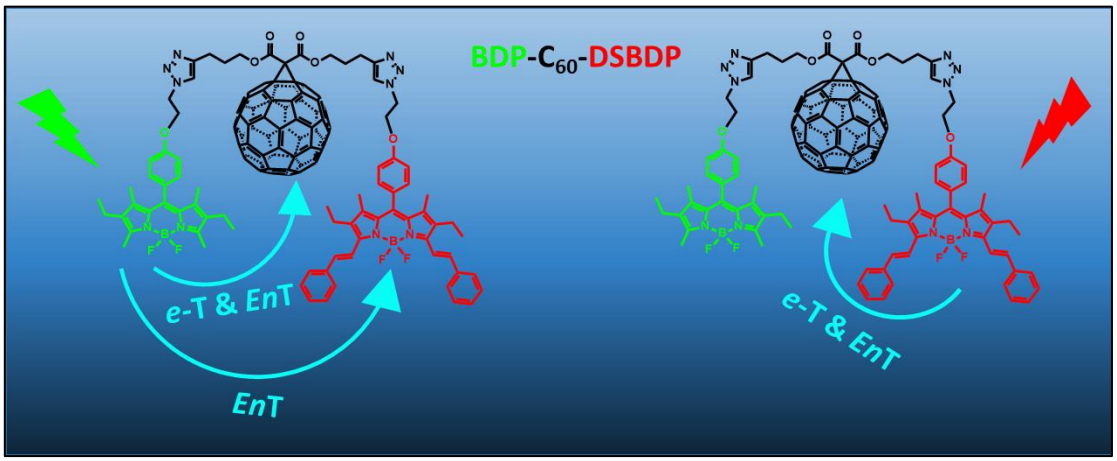

Graphical Abstract

Abstract: Photoinduced electron and energy transfer pathways are elucidated in a panchromatic light-absorbing, covalently linked triad (BODIPY-C_{60}-distyryl-BODIPY, noted as BDP-C_{60}-DSBDP) along with the two reference dyads: BODIPY-C_{60} (BDP-C_{60}) and distyryl-BODIPY-C_{60} (DSBDP-C_{60}). The flexible linker between the BODIPY and C_{60} units leads to different possible conformations with varying donor-acceptor distances. Ultrafast transient absorption along with the time-resolved emission spectroscopies revealed the occurrence of different photoinduced electron/energy transfer processes in these conformers. Photoexcitation of the BODIPY units in the two reference dyads leads to one electron and two energy transfer steps from BODIPY to C_{60}. However, in the BDP-C_{60}-DSBDP triad, additional energy transfer processes from BDP to DSBDP were evidenced upon photoexcitation of the BDP unit. The singlet excited state of DSBDP in the triad then follows the same relaxation route as that of the DSBDP-C_{60} dyad. The intricate photophysics, particularly the formation of radical ion pairs in these flexible covalently linked donor-acceptor systems contribute to our fundamental understanding of electron and energy transfer mechanisms, which is important to build donor-acceptor assemblies for energy applications.

1. Introduction

Understanding photoinduced processes is of particular importance for the design of molecular systems for diverse applications such as in artificial photosynthesis, photovoltaics, molecular electronics and photonics [1-9]. A large number of elegant donor-photosensitizer-acceptor (D-P-A) and photosensitizer-acceptor (P-A) systems have been designed and extensively studied [6-12]. Apart from the classical chromophores such as porphyrins and phthalocyanines, the use of BODIPYs as photosensitizer or electron/energy donor is promising in the light of its photophysical properties. Their attractive properties including strong visible-light absorption, photo-stability, high fluorescence quantum yields and facile optical and electrochemical tunability [5,13,14] are crucial to build innovative D-A systems. Remarkably, BODIPYs can be employed as electron/energy donor or acceptor based on the counter molecular entity [15,16]. Furthermore, fullerenes and their derivatives have also been largely studied in artificial photosynthetic systems due to their outstanding electrochemical properties and low reorganization energy in electron transfer processes [17,18]. Over the years, scores of reported BODIPY-C_{60} based donor-acceptor systems have illustrated the photoinduced electron transfer leading to the charge-separated state (BODIPY$^{\cdot+}$-$C_{60}^{\cdot-}$) [19-24].

Certainly, broad-spectrum light capture is vital for the realization of artificial photosynthesis and therefore much efforts have been made to cover the entire visible range absorption of photosensitizers. For this purpose, Obondi and coworkers have investigated a series of bis(styryl)-BODIPY-C_{60} assemblies featuring a wide-band light capture on account of extended conjugation of the BODIPY core [15]. Another strategy is to use multichromophoric systems as reported in the subphthalocyanine-azaBODIPY-C_{60} triad in which competitive ultrafast electron transfers were observed due to the V-configured system [25]. D'Souza and coworkers have also reported broadband capturing, BODIPY-Porphyrin-C_{60} triads and demonstrated different photoinduced processes depending on the excitation wavelengths [26,27]. Several panchromatic supramolecular systems containing multiple BODIPY chromophores linked to C_{60} moiety were developed capable of mimicking the photosynthetic 'antenna-reaction centre' [28,29]. However, to the best of our knowledge, very few reports are available on covalently linked multiple BODIPY-fullerene systems highlighting ultrafast photoinduced processes [29]. Recently, Allard *et al.* synthesized a novel broadband absorbing multiple BODIPY-C_{60} covalently linked triad (300-750 nm) having a distinct design rationale [30]. The two different BODIPYs, a BODIPY (BDP) and a more conjugated distyryl-BODIPY (DSBDP), are linked to the two sides of the methanofullerene platform using a facile stepwise or one-pot synthesis process to build the BDP-C_{60}-DSBDP triad (Scheme 1). The selective population of the triplet-excited state in this triad and the two reference dyads (BDP-C_{60} and DSBDP-C_{60}) has recently been reported by our group using nanosecond transient absorption spectroscopy [31]. In the triad, the localization of the long-lived triplet excited state (280 µs) on ^{3}DSBDP*, regardless of the excitation wavelength makes this system interesting in the field of wideband light-capturing heavy atom free triplet photosensitizer. However, the early steps of the relaxation pathways leading to the formation of the triplet states in the two dyads and the BDP-C_{60}-DSBDP triad (Scheme 1) were not investigated.

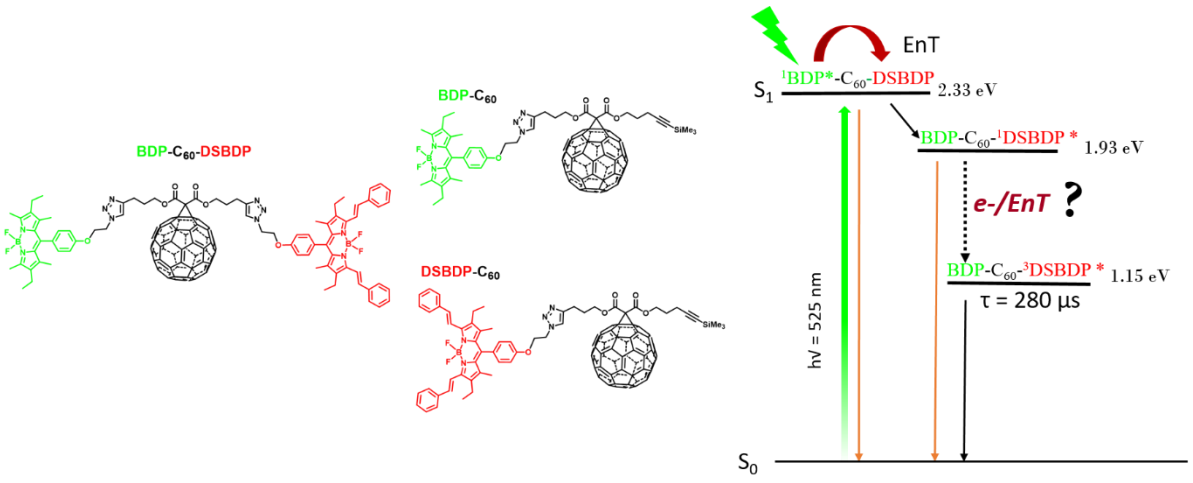

Scheme 1. Structures of the BDP-C_{60}-DSBDP triad and the two reference BDP-C_{60} and DSBDP-C_{60} dyads under investigation and simplified scheme of the processes leading to the formation of the ^{3}DSBDP* state in the triad.

In the present study, we have systematically investigated the photoinduced electron and energy transfer processes in the two reference dyads and the triad. The flexible linker between the BODIPY and fullerene units allows various possibilities of donor-acceptor distances in different conformations, leading to a complex dynamics of photoinduced processes. Combining the results of ultrafast spectroscopy, steady-state and time-resolved fluorescence studies, we present herein the complete relaxation pathways in these systems. Details of photoinduced

electron and energy processes, in particular the formation of radical pairs in this multiple chromophoric donor-acceptor compound are important for designing strategies for artificial photosynthetic systems.

2. Materials and methods

2.1 Materials

All the molecular systems (BDP, DSBDP, methanofullerene platform, BDP-C_{60}, DSBDP-C_{60} and BDP-C_{60}-DSBDP) were synthesized in the Institut Lavoisier de Versailles following the procedures described by Allard *et al* [30].
Spectroscopic grade benzonitrile and dichloromethane were purchased from Sigma-Aldrich and used without further purification.

2.2 Steady-state absorption and fluorescence spectroscopy

The UV-visible ground state absorption spectra were recorded with a UV-2600 spectrophotometer (Shimadzu). Emission spectra were measured using Scientific Fluoromax PLUS (Horiba Jobin-Yvon). The concentrations of the samples used for absorption and emission measurements were in the micro-molar range and the spectra were recorded in 1 cm optical path quartz cells.

2.3 Time-correlated single-photon counting

Time-resolved fluorescence measurements were performed using the set-up previously described in the literature [32]. The BODIPY moieties in the dyads and the triad were excited using two excitation wavelengths (495 or 635 nm). Using a Ti:sapphire laser (Coherent Chameleon Ultra II, 80 MHz) coupled to a pulse picker (4 MHz) and a harmonic generator (SHG/THG, APE), 495 nm femtosecond excitation pulses (<200 fs, FWHM, 4 MHz) were employed to excite the BDP-C_{60} dyad and the triad. The DSBDP-C_{60} dyad and the triad were excited using a 635 nm picosecond excitation pulse (Picoquant laser diode) emitting with a pulse width <90ps (FWHM) and a repetition rate of 8 MHz. Fluorescence emission was recorded at two specific wavelengths, 535 nm and 655 nm, corresponding to the emission of BDP and DSBDP units respectively, using a FluoTime 200 spectrometer (4-nm bandpass) with polarizers at a magic angle. Fluorescence decays were then collected until a maximum of 10000 counts was attained using a PicoHarp 300 TCSPC system (bin time = 4ps). The analyses of emission decay data were done with a weighted sum of exponential decays convolved by the IRF signal measured in a light-scattering Ludox colloidal solution, using the FluoFit software (PicoQuant). The full width at half maximum (FWHM) of IRF at 495 and 635 nm excitations was equal to 40 ps and 90 ps, respectively, which can be considered as the time-resolution of the measurements. Solutions with an absorbance below 0.1 (1 cm path-length) at excitation wavelengths were used. The quality of the fits was assessed by the value of χ^2 (<1.1), the weighted residuals and their autocorrelation function.

2.4 Spectroelectrochemistry

Spectroelectrochemical measurements were performed with the help of an optically transparent thin layer electrochemical cell (OTTLE) connected with a PalmSens4 potentiostat. The cell employs a platinum mesh as a working electrode, a platinum wire as a counter electrode and a silver wire as a quasi-reference electrode. 0.1 M of hexafluorophosphate tetrabutylammonium ($TBAPF_6$) was used as a supporting electrolyte in dichloromethane. The spectra were recorded in Varian 5000 Cary spectrophotometer. The concentration of DSBDP in dichloromethane solution was 0.2 mM.

2.5 Femtosecond transient absorption

Femtosecond UV-Vis-NIR spectra were recorded using a commercial set-up (Ultrafast systems, Helios) [33]. The fundamental 800 nm beam was split into two beams to generate (a) a pump (λ_{exc} = 525 and 640 nm) in the optical parametric amplifier and (b) probe pulses, a white light continuum in the UV-Vis-NIR range (300 to 1400 nm), using either a CaF_2 plate (330-660 nm) or a sapphire plate (440-780 nm) or a YAG crystal (830-1400 nm). The pump energy was 2 μJ per pulse (beam size of 250 μm FWHM). The spectra were recorded in a 2 mm path length quartz cell under continuous stirring using a Teflon-coated bar. All measurements were performed in argon degassed solutions at room temperature. All the samples were scanned bi-directionally to ensure data reproducibility. The transient absorption data were corrected for the chirp of the white-light continuum using the Surface Xplorer program, supplied by the Ultrafast systems. The instrument response function (IRF) was around 200 fs (FWHM). Notably, due to the strong benzonitrile solvent contribution within 2 ps time windows, a precise assignment of the shortest lifetime close to 1 ps could not be ascertained.

3. Results and discussion

3.1 Steady-state absorption and emission

The steady-state absorption and emission studies of the triad and the two reference dyads have recently been reported [31]. Briefly, the BDP-C_{60} and DSBDP-C_{60} dyad absorption spectra show maxima at 535 and 637 nm identical to those of the parent BDP and DSBDP moieties respectively (Fig.1a and b). Further, a strong band at 330 nm and a small sharp band at 428 nm correspond to the absorption of the methanofullerene platform. The absorption spectrum of the BDP-C_{60}-DSBDP triad (Fig. 1c) overlaps well with the sum of the absorption spectra of BDP, DSBDP and C_{60} [31]. Therefore, these observations infer a negligible communication between the two BODIPY photosensitizers and the C_{60} acceptor units in the electronic ground state [31]. The ground state absorption of the triad shows a good coverage in the entire visible range due to the presence of two differently functionalized BODIPY units along with the C_{60} moiety (Fig.1c).
Upon excitation at 495 nm and 605 nm respectively, the two BDP-C_{60} and DSBDP-C_{60} dyads show a significant quenching of the fluorescence intensities as compared to their parent BODIPYs (quantum yield decrease of 98 and 92 %, respectively). These observations suggest efficient energy and/or electron transfer events from the BODIPY excited state to the fullerene moiety [31]. The steady-state fluorescence spectrum of the triad after the excitation of the BDP unit (λ_{exc} = 495 nm) reveals two emission bands with maxima at 537 nm and 650 nm corresponding to the emission of BDP and DSBDP respectively. The intensity of the 537 nm emission band of the BDP in the triad is more strongly reduced (quantum yield decrease of over 99%) as compared to the BDP-C_{60} dyad. The significant emission quenching of BDP points out the photoinduced processes similar to those observed in the case of the BDP-C_{60} dyad with an additional energy transfer from ^{1}BDP* to DSBDP as previously demonstrated [31]. Further, this was confirmed by recording the excitation spectrum of the triad at the emission of DSBDP moiety (λ_{em} = 670 nm). The excitation spectrum revealed the contribution of the BDP moiety (λ_{abs} = 525 nm) in addition to that of DSBDP (λ_{abs} = 637 nm (SI Fig 1.) [31].

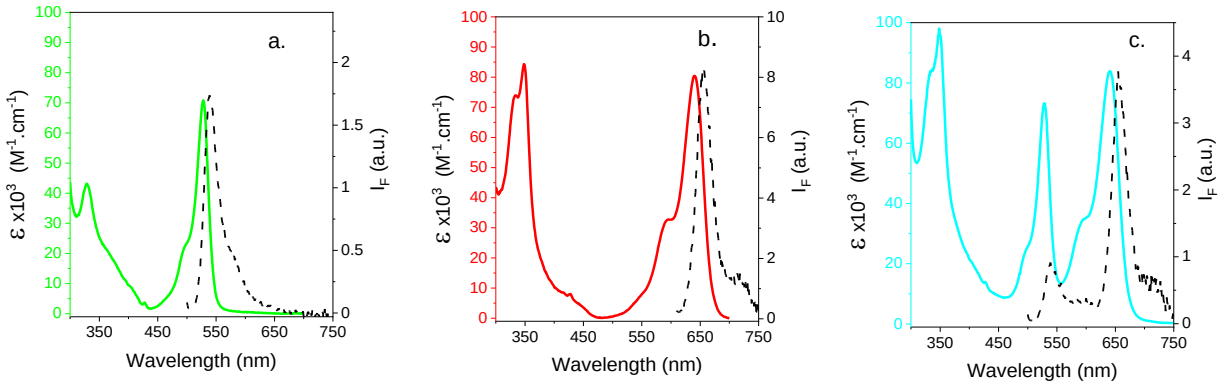

Fig.1. UV-Visible absorption and emission spectra of a. BDP-C_{60} dyad (λ_{exc} = 495 nm), b. DSBDP-C_{60} dyad (λ_{exc} = 605 nm) and c. BDP-C_{60}-DSBDP triad (λ_{exc} = 495 nm) recorded in benzonitrile.

3.2 Spectroelectrochemical measurements (SEC)

The electrochemical properties of the dyads and the triad were previously studied by cyclic voltammetry [30]. To help assign the spectroscopic transient signals, spectroelectrochemical measurements were performed on DSBDP and BDP. The measurements were carried out in dichloromethane since these compounds display an entirely reversible oxidation process in this solvent. Spectral changes owing to one-electron oxidation of BDP were recorded at varying oxidation potentials (1 to 1.3 V) are shown in Fig. 2a. The SEC spectra of oxidized BDP radical cation ($BDP^{\cdot+}$) reveal a new band at 415 nm. Further, the SEC absorption bands for one-electron oxidized DSBDP radical cation ($DSBDP^{\cdot+}$) show up at 429, 458, 542 nm and an intense band at 680 nm upon gradually increasing the oxidation potential from 0.7 to 1.1 V (Fig. 2b). Also, the SEC absorption spectra of one electron reduced fullerene moiety ($C_{60}^{\cdot-}$) was previously reported, showing a sharp absorption band at about 1035 nm.

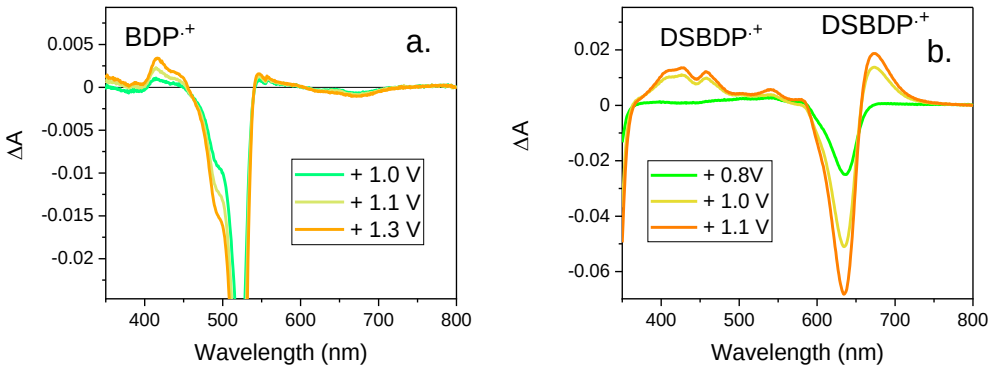

Fig. 2. a. Difference absorption spectra relative to the neutral state of one electron oxidized a. BDP (242 µM) and b. DSBDP (192 µM) with 0.1 M $TBAPF_6$ in dichloromethane solution showing the rise of $BDP^{\cdot+}$ and $DSBDP^{\cdot+}$ respectively, upon gradually increasing the oxidation potential. The negative bands correspond to the depletion of the electronic ground state.

3.3 Time-resolved emission

To probe the kinetics of photophysical processes from excited BODIPYs to C_{60}, time-correlated single-photon counting studies were performed upon photoexcitation of BODIPY units in the two dyads and the triad. The fluorescence decay profiles are presented in Fig. 3 and the corresponding lifetimes are detailed in Table 1. In benzonitrile, the excitation of BDP and DSBDP units leads to a monoexponential fluorescence decay giving a lifetime of 4.57 and 4.46 ns, respectively [31], typical of the BODIPY singlet excited state [34]. However, the fluorescence decays of BDP and DSBDP in the two dyads are more complex and are satisfactorily fitted with three exponentials.

Multiple time constants obtained in a similar reported BODIPY-C_{60} dyad were attributed to the presence of different conformations due to the flexible linker between donor-acceptor moieties [24]. The flexibility allows for different donor-acceptor distances and therefore photoinduced processes (electron and/or energy transfer) of different kinetics are possible in such assemblies. The two short lifetimes of the order of hundred picoseconds with high contributions in the two dyads can be attributed to the energy or electron transfer processes in conformers with relatively short donor-acceptor distances. Furthermore, the long lifetime of several nanoseconds with a very small contribution (less than 1%) can be due to an extended conformer with negligible interaction between the BODIPY and C_{60} units, as previously reported in a flexible porphyrin-fullerene dyad [35].

Upon exciting the BDP unit in the BDP-C_{60}-DSBDP triad (λ_{exc} = 495 nm), the decay of the BDP unit (λ_{em}= 535 nm) can be satisfactorily fitted with a four exponential model. The three short components can be related to electron or energy transfer processes from ^{1}BDP* to C_{60} as in the BDP-C_{60} dyad, in addition to a supplement excitation energy transfer from ^{1}BDP* to DSBDP in a conformer with a short BDP-DSBDP distance. Furthermore, a very low contribution of the nanosecond lifetime (<1%) can be again associated with an extended conformer with a long distance between BDP and both the DSBDP and C_{60} moieties. On the other hand, the decay of the DSBDP unit (λ_{em} = 650 nm) at the same excitation can be satisfactorily fitted by three time constants which are similar to those obtained in the DSBDP-C_{60} dyad. Similarly, fitting the fluorescence decay of the DSBDP unit upon excitation of DSBDP at 635 nm also yields almost similar time constants with analogous contributions as that in the DSBDP-C_{60} dyad (see Table 1). These observations indicate that ^{1}DSBDP* once formed after excitation energy transfer from ^{1}BDP* in the triad or from a direct excitation follows the same relaxation pathways as that of ^{1}DSBDP* in the DSBDP-C_{60} dyad.

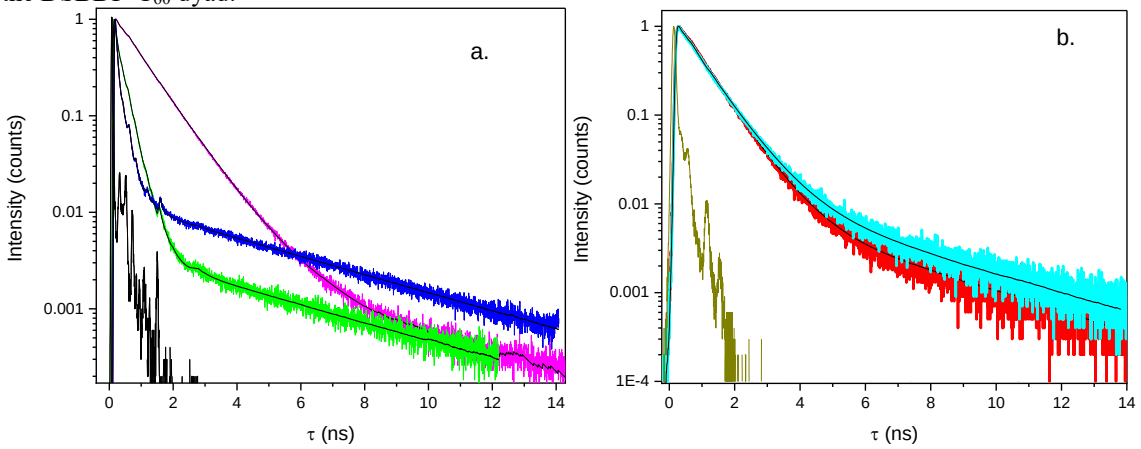

Fig. 3. Fluorescence decay profiles obtained by TCSPC of a. BDP-C_{60} dyad (green, λ_{exc} = 495 nm, λ_{em} = 535 nm – BDP emission), BDP-C_{60}-DSBDP triad (blue, λ_{exc} = 495 nm, λ_{em} = 535 nm - BDP emission; pink, λ_{exc} = 495 nm, λ_{em} = 650 nm – DSBDP emission) and b. DSBDP-C_{60} dyad (red, λ_{exc} = 635 nm, λ_{em} = 650 nm – DSBDP emission), and BDP-C_{60}-DSBDP triad (cyan, λ_{exc} = 635 nm, λ_{em} = 650 nm – DSBDP emission) in benzonitrile. Grey and dark green curves represent measured IRF signals at 495 and 635 nm excitations, respectively.

Table 1. Fluorescence lifetimes (contribution in %) in benzonitrile are expressed in nanoseconds with an error of ± 40 ps and ± 80 ps for 495 and 635 nm excitation, respectively, the longest lifetime was fixed with that of the parent BODIPYs, [a] λ_{exc} = 495 nm, λ_{em}= 535 nm, [b]λ_{exc} = 635 nm, λ_{em}= 650 nm, [c]λ_{exc} = 495 nm, λ_{em}= 650 nm

Molecule	τ_1 (amplitude, wt.%)	τ_2 (amplitude, wt.%)	τ_3 (amplitude, wt.%)	τ_4 (amplitude, wt.%)
BDP[a]	4.57	--	--	--
BDP-C_{60}[a]	0.04 (39.19%)	0.23 (60.57%)	4.57 (0.25%)	--
DSBDP[b]	4.46	--	--	--
DSBDP-C_{60}[b]	0.15 (25.82%)	0.73 (73.11%)	4.46 (1.06%)	--
DSBDP-C_{60}-BDP[a]	0.02 (59.7%)	0.09 (37.77%)	0.225 (5.4%)	4.57 (0.40%)
DSBDP-C_{60}-BDP[b]	0.18 (28.18%)	0.79 (70.15%)	4.46 (1.34%)	--
DSBDP-C_{60}-BDP[c]	0.33 (28%)	0.88 (70%)	4.46 (0.80%)	--

3.4 Femtosecond transient absorption spectroscopy

Femtosecond transient absorption (TA) spectra were recorded to characterize the early photophysical events taking place in the BDP-C_{60}-DSBDP triad and the two associated dyads (BDP-C_{60} and DSBDP-C_{60}) upon selective excitation of chromophore units. At the outset, TA spectra are detailed for BDP-C_{60} and DSBDP-C_{60} dyads by selectively exciting the BDP and DSBDP units at 525 and 640 nm, respectively in benzonitrile. Then, the BDP-C_{60}-DSBDP triad TA spectra are recorded at the same selective excitation wavelengths.

3.4.1 BDP-C_{60} dyad

Femtosecond transient absorption spectra of the BDP-C_{60} dyad were recorded over a range of 330-1450 nm, detailed in four different time windows until 2460 ps (Fig. 4). During very short pump-probe delays from -0.3 ps to 0.4 ps, as depicted in Fig. 4a, the rising of positive signals at 344, 427 nm in visible and at 1278 nm in the NIR region is coupled with a negative broad absorption band at about 495-550 nm. This negative transient absorption band is associated with the depopulation of the BDP ground state and BDP stimulated emission (inverted absorption and emission spectra in black and grey curves respectively are shown in Fig. 4a). These spectral features are characteristic of the formation of ^{1}BDP* as already observed in a formerly reported BODIPY-C_{60} dyad [24]. Moreover, the rising of another transient absorption band at 1045 nm is associated with the formation of $C_{60}^{\cdot-}$ ($C_{60}^{\cdot-}$ signature obtained by SEC shown in Fig. 4a; pink curve) [24], suggesting an ultrafast electron transfer within the IRF, from the Franck-Condon zone of ^{1}BDP* to C_{60}.

Then, from 0.5 to 100 ps, the increase and narrowing of the $C_{60}^{\cdot-}$ band in the NIR region can be explained by a vibrational cooling of $C_{60}^{\cdot-}$. Furthermore, a decay in ^{1}BDP* signals is coupled with a rise of a new band at 916 nm which is attributed to the $^1C_{60}^*$ absorption (the $^1C_{60}$* reference spectrum is shown as a black curve in Fig. 4c) [36]. This is related to an energy transfer from ^{1}BDP* to C_{60}.

The third temporal window from 100 ps to 300 ps exhibits a subsequent decrease in ^{1}BDP* absorption together with the ground state recovery and a second rise of the band at 916 nm of $^1C_{60}$* while the band at 1045 nm related to $C_{60}^{\cdot-}$ remains constant (Fig. 4c). It should be noted that the absorption spectra of both the species ($^1C_{60}$* and $C_{60}^{\cdot-}$) largely overlap in the NIR region. Thus, this behaviour suggests a charge recombination process causing the depopulation of $C_{60}^{\cdot-}$ with a simultaneous population of the $^1C_{60}$* due to a second energy transfer.

In the final time window above 300 ps, the bands for ^{1}BDP* and $^1C_{60}$* decay, and a new band rises at 710 nm which is attributed to $^3C_{60}$* (see the dark green reference spectrum in Fig. 4d) [24,31]. The formation of $^3C_{60}$* is explained by an intersystem crossing from the $^1C_{60}$*.

Kinetic traces at some specific wavelengths representing the transient species described above are presented in SI Fig. 2. The chosen probe wavelengths at 427, 490, 550 and 1278 nm correspond to ^{1}BDP*. 916 and 1045 nm

represent $^1C_{60}$* and $C_{60}^{\cdot-}$ while 710 nm corresponds to the triplet excited state of C_{60} [18,31]. These kinetic traces can be satisfactorily fitted by a four exponential model and the time constants obtained are summarized in SI Table 1. Further, global fitting analyses of kinetic traces in Fig. 5a converged with five exponentials (<1 ps, 5 ps, 42 ps, 197 ps, 1.4 ns). These time constants are similar to those obtained by the fit of single time traces. Alongside, decay associated difference spectra (DADS) obtained by global fitting of kinetics are shown in Fig. 5b.

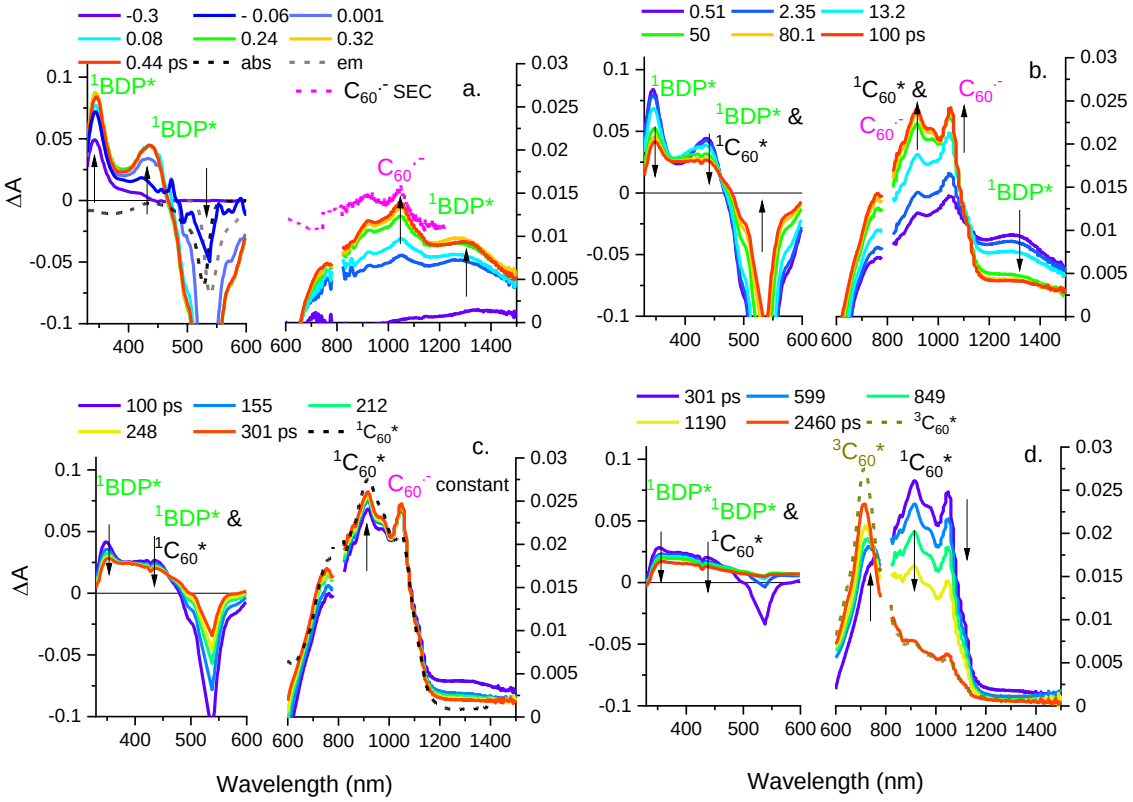

Fig. 4. Femtosecond transient absorption spectra of BDP-C_{60} at specified delay times: a. -0.3 to 0.44 ps; b. 0.51 to 100 ps; c. 100 to 301 ps and d. 301 to 2460 ps in deaerated benzonitrile. λ_{exc} = 525 nm. The grey and black curves in panel (a) represent the respective steady-state absorption (abs) and emission (em) spectra of pristine BDP.

The time constant of < 1 ps obtained in the fitting of the kinetics at characteristic probe wavelength of 1045 nm as well as in the global fitting (see SI Table 1 and DADS in Fig. 5b) is attributed to the ultrafast formation of C_{60} radical anion. Then, the time constant of about 5 ps obtained by global fitting is interpreted as vibrational cooling of $C_{60}^{\cdot-}$, initially formed with excess energy. Furthermore, the 42 ps and 197 ps time components appear as decay times in the fitting of the time traces corresponding to the ^{1}BDP* and as rising times in the fitting of those of $^1C_{60}$*. These time constants are also close to the fluorescence lifetimes obtained by TCSPC (40 and 230 ps, Fig. 2 and Table 1). Therefore, these observations can be associated with energy transfer processes from ^{1}BDP* to C_{60} occurring in two BDP-C_{60} conformers. From the DADS shown in Fig. 5b, the 42 ps time constant can also be related to the charge recombination (positive band of $C_{60}^{\cdot-}$ at 1045 nm and of $BDP^{\cdot+}$ at 415 nm). Finally, the 1.4 ns time constant is attributed to the intersystem crossing (ISC) from $^1C_{60}$* to $^3C_{60}$* (positive band of $^1C_{60}$* at 916 nm and a negative band of $^3C_{60}$* at 710 nm in DADS). The population of $^3C_{60}$* was confirmed by nanosecond transient absorption measurements (SI Fig. 3a) in agreement with the recent report [31]. Fig. 6 summarizes the photoinduced electron or energy transfer processes in the BDP-C_{60} dyad. Different photoinduced processes can be related to different families of conformers that were already observed for a similar dyad [24]. It is to be noted that the analyses were complex since $C_{60}^{\cdot-}$ and $^1C_{60}$* show very similar absorption features in the NIR region. Therefore, the electron/energy transfer processes in each family of conformers highlight the dominant relaxation pathways. The ultrafast electron transfer process (<1 ps) is associated with a conformer with the shortest distance between BODIPY and C_{60} units (named Conformer 1). Further, the two energy transfer processes occurring in about 40 and 200 ps are related to the two conformers (named Conformers 2 and 3 respectively), with intermediate donor-acceptor distances. Conformer 1 connotes a short D-A distance, undergoing ultrafast electron transfer. Conformers 2 and 3 with intermediate donor-acceptor distances undergo energy transfer from ^{1}BDP* to C_{60}. In addition, it should be reminded that a conformer with a long distance between BDP and C_{60} (named conformer 4) with nanosecond fluorescence lifetime was observed due to negligible electron and energy transfer processes.

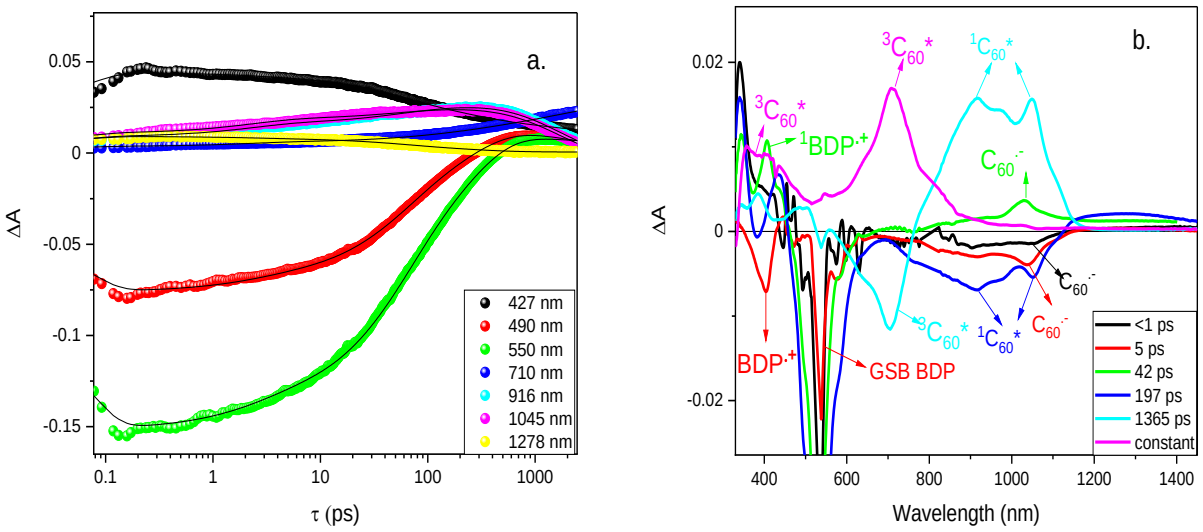

Fig. 5 a. Global fit of kinetic traces of BDP-C_{60} dyad using multi-exponential model and b. decay associated difference spectra (DADS) obtained by a global fit of femtosecond transient spectra of the BDP-C_{60} dyad.

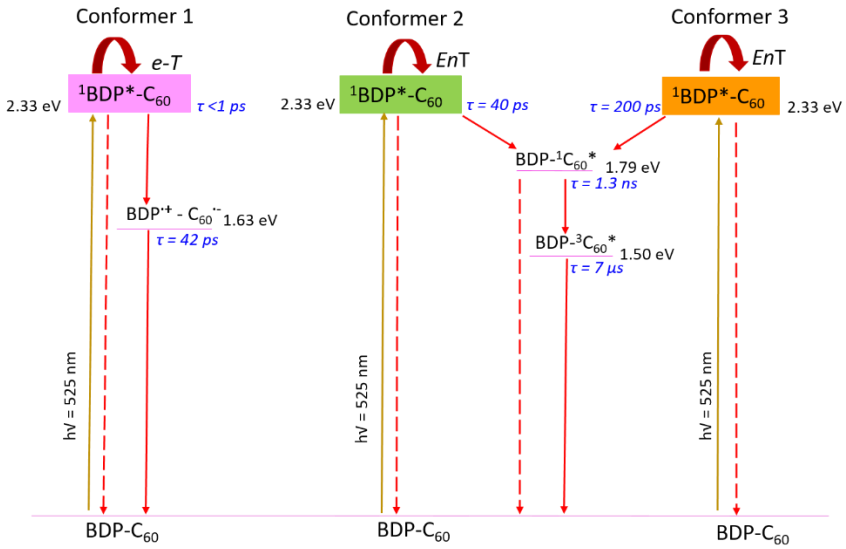

Fig. 6. Energy level diagram showing the photoinduced processes in the BDP-C_{60} dyad. Conformer 1 connotes a short D-A distance, undergoing ultrafast electron transfer. Conformers 2 and 3 with intermediate donor-acceptor distances undergo energy transfer from ^{1}BDP* to C_{60}. The indicated lifetimes represent the kinetics of the dominant relaxation processes. Note: For the sake of simplicity, an extended conformer with no electron/energy transfer process is not shown in the scheme.

3.4.2 DSBDP-C_{60} dyad

First, femtosecond transient absorption measurement was performed for the parent DSBDP upon excitation at 640 nm (SI Fig. 4). Similar transient spectra were observed at all delay times corresponding to only one excited stated ^{1}DSBDP*. The transient spectra show two negative bands at 640 and 720 nm which correspond to the ground state bleach and the stimulated emission, respectively as well as excited state absorption bands at 455, 855 and 1000 nm. The fitting of kinetic traces (SI Fig. 4) gives two time constants of (0.9 ± 0.1) ps and (4 ± 1) ns, which are attributed to the vibrational cooling followed by the relaxation of the singlet excited state.

Upon exciting DSBDP unit of the DSBDP-C_{60} dyad at 640 nm, the femtosecond transient absorption spectra also exhibit the rise of bands at 455, 855 and 1000 nm until 0.4 ps (Fig. 7a). These spectral features are the same as the spectrum of the parent DSBDP at 0.4 ps (dashed, blue curve in Fig. 7a), therefore supporting the selective excitation of the DSBDP unit at 640 nm and the formation of ^{1}DSBDP*.

From 0.4 ps to 20 ps, the decay of the ^{1}DSBDP* band at 455 nm is accompanied by the concomitant rise of new bands at about 687 and 1045 nm. The band at 1045 nm corresponds to the absorption of the C_{60} radical anion as previously shown in the BDP-C_{60} dyad study. The one at 687 nm is attributed to the DSBDP radical cation (DSBDP$^{\cdot+}$), since its absorption corresponds to the DSBDP$^{\cdot+}$ signature obtained by spectroelectrochemistry

(DSBDP$^{\cdot+}$ SEC in Fig. 7b; dashed, brown curve) and the chemical oxidation of DSBDP-C_{60} dyad with $FeCl_3.6H_2O$ (SI Fig. 5). This observation suggests the photoinduced electron transfer from ^{1}DSBDP* to C_{60}.

In the third time regime from 20 to 300 ps (Fig. 7c), charge-separated state bands at 687 and 1045 nm decay, indicating the charge recombination process. Moreover, the bands at 455, 855 and 1000 nm continue to decrease and can be related to additional photoinduced energy transfer processes from ^{1}DSBDP* to C_{60}. However, the rising band of $^1C_{60}$* can not be observed due to the spectral overlap of the two decay species ^{1}DSBDP* and $C_{60}^{\cdot-}$ with that of the rising of $^1C_{60}$* in NIR (800-1000 nm).

In the final time panel above 300 ps (Fig. 7d), the transient bands corresponding to ^{1}DSBDP* continue to decay. An additional shoulder is still observed above 1000 nm that could be assigned to the spectrum of $^1C_{60}$*. At the last delay time, transient bands at about 710 and 1050 nm are observed. As shown by the reference spectra of $^3C_{60}$* obtained from femtosecond TA measurement of pristine C_{60}-platform at 2.4 ns and of ^{3}DSBDP* from nanosecond TA at 5 ns in Fig. 7d, these bands could be assigned to the formation of both $^3C_{60}$* and ^{3}DSBDP* at the end of probed time-window. The formation of $^3C_{60}$* is explained by inter-system crossing from $^1C_{60}$*.

Nanosecond transient absorption measurement with a selective excitation of DSBDP unit at 640 nm revealed transient absorption bands corresponding to ^{3}DSBDP* (SI Fig. 3b, red curve) and the kinetics could be fitted mono-exponentially without any contribution of $^3C_{60}$* lifetime. These observations have already been detailed previously [31]. Therefore, although a mixture of ^{3}DSBDP* and $^3C_{60}$* was observed at the end of the femtosecond measurement window, the final excited state is ^{3}DSBDP* populated from an energy transfer from the higher energy $^3C_{60}$*. These findings point out the ping-pong energy transfer between C_{60} and DSBDP as already observed by Huang *et al* [37].

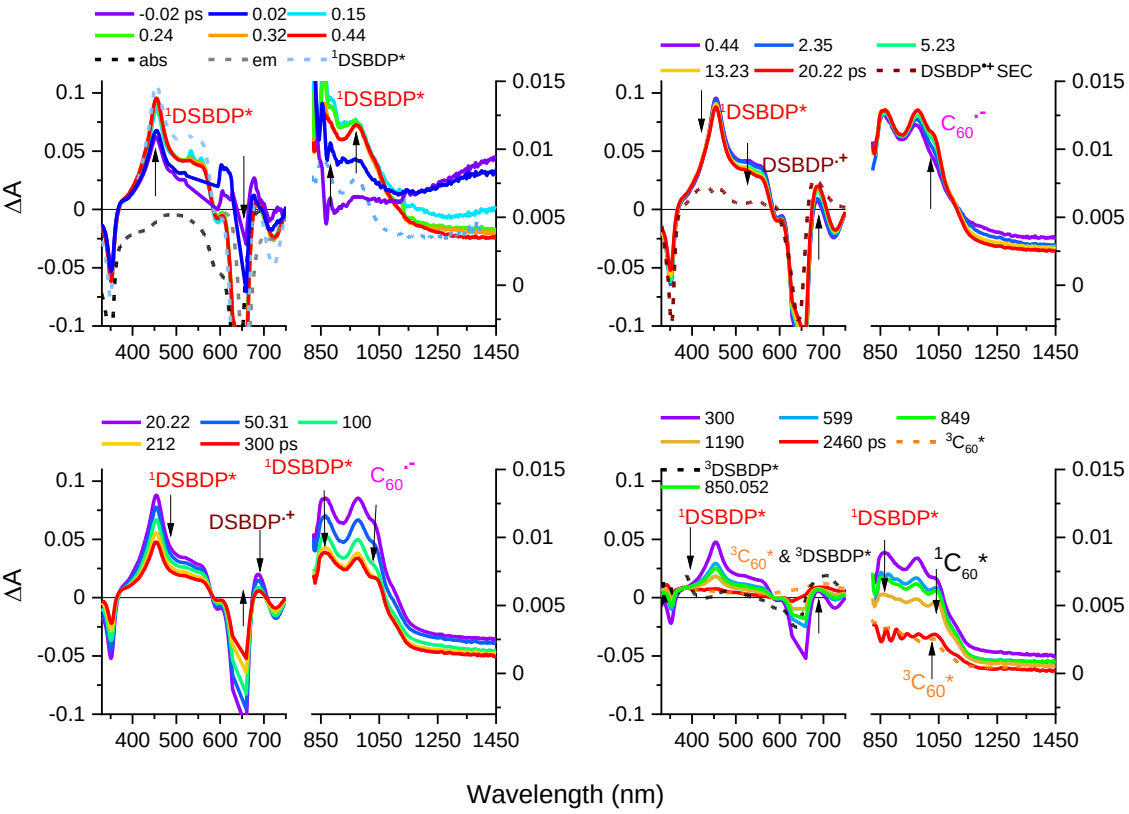

Fig. 7. Femtosecond transient absorption spectra of DSBDP-C_{60} at specified delay times: a. -0.02 to 0.44 ps; b. 0.44 to 20 ps; c. 20 to 300 ps and d. 300 to 2460 ps in solvent benzonitrile. λ_{exc} = 640 nm. The dashed grey and black curves in panel (a) represent the respective steady-state absorption (abs) and emission (em) spectrum of pristine DSBDP.

As with the BDP-C_{60} dyad, the kinetic fitting was performed at several specific wavelengths corresponding to the absorption of the transient species. The attribution of the transient species relative to these wavelengths is summarized in SI Table 2 and their corresponding transient kinetics are shown in SI. Fig. 5. Time constants obtained from the individual multi-exponential fit are in agreement with the global multi-exponential fit shown in Fig. 8a. Three exponential model satisfactorily fit the kinetic traces yielding the time constants of 4, 87 and 874 ps. The DADS (Fig. 8b) of the first component of 4 ps shows the negative bands at 687 and 1045 nm corresponding to the rise of DSBDP$^{\cdot+}$ and $C_{60}^{\cdot-}$ absorption, respectively. Similar time constants are also observed in the individual fitting of the decay of ^{1}DSBDP* and the rising of charge-separated state absorption. As in the BDP-C_{60} dyad with

the same flexible linker, different donor-acceptor distances are also possible in this dyad. The first time constant is therefore related to the formation of the charge-separated state in a short DSBDP-C_{60} distance conformer (named Conformer 1, Fig. 9). It should be noted that, unlike the BDP-C_{60} dyad, no ultrafast electron transfer (<1 ps) from ^{1}DSBDP* to C_{60} was observed. This can be explained by the fact that the electron transfer is less thermodynamically favourable in the DSBDP-C_{60} dyad (ΔGcs = -0.54 eV versus -0.70 eV for the BDP-C_{60} dyad). The DADS of the second time constant (87 ps) presents the decay of the charge-separated state species corresponding to the charge recombination. Furthermore, in the same DADS, a decay of ^{1}DSBDP* is also observed. It can be related to a parallel process of energy transfer in a second conformer with an intermediate distance between DSBDP and C_{60} (named Conformer 2, Fig. 9). This time component is in a decent agreement with the fluorescence lifetime of ^{1}DSBDP* (τ_1 = 150 ps, Fig. 3. and Table 1).
The DADS of the last time constant of 874 ps exhibits a decay feature of ^{1}DSBDP* with typical absorption at 455 nm. This decay time agrees well with the results of the individual fit (SI. Table 2) as well as with the fluorescence lifetime of 730 ps (Fig. 3 and Table 1). Simultaneously, a negative band in DADS at about 916 nm corresponds to the rise of $^1C_{60}$*, indicating a second energy transfer from ^{1}DSBDP* to C_{60} in a more extended conformer (named Conformer 3). In addition, the DADS also presents a rising of $^3C_{60}$* and ^{3}DSBDP* features at the 700 nm region, which are in agreement with the rising component in the individual fits (see 687 nm fit of SI Table 2). This can be related to the formation of both $^3C_{60}$* and ^{3}DSBDP* by the ping-pong mechanism as previously explained. Figure 9 puts forward all the dominant photo-induced processes in the DSBDP-C_{60} dyad.

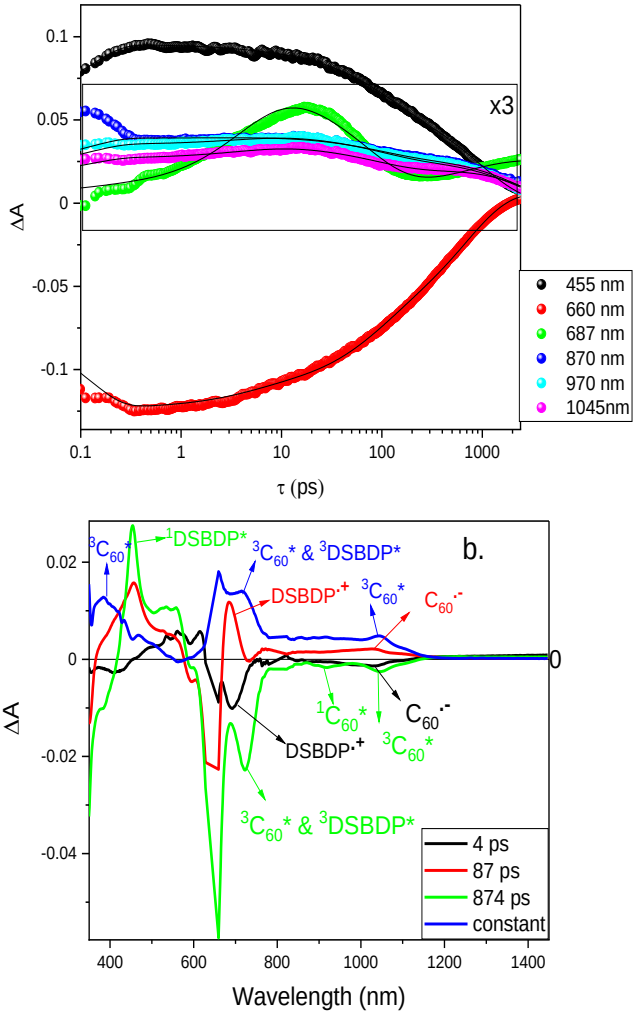

Fig. 8. a. Global fit of kinetic traces using three exponential model and b. Decay associated difference spectra (DADS) obtained by global fit of femtosecond transient spectra of the DSBDP-C_{60} dyad. Note: The kinetics traces from 687 nm to 1045 nm are amplified by 3 times for better visibility.

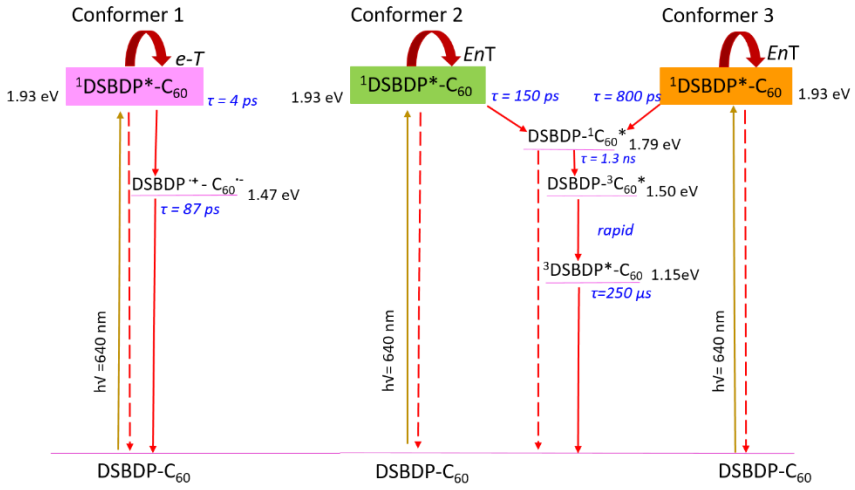

Fig. 9. Energy level diagram presenting the photoinduced processes in DSBDP-C_{60} dyad in argon-saturated benzonitrile. Conformer 1 connotes a short D-A distance, undergoing rapid electron transfer. Conformers 2 and 3 with intermediate donor-acceptor distances undergo photo-excitation energy transfer from ^{1}DSBDP* to C_{60}. The indicated lifetimes represent the kinetics of the dominant relaxation processes. Note: For the sake of simplicity, an extended conformer with no electron/energy transfer process is not shown in the scheme.

3.4.3 BDP-C_{60}-DSBDP triad

The femtosecond TA spectra of the DSBDP-C_{60}-BDP triad at the excitation wavelength of 525 nm corresponding to the absorption of BDP are shown in Fig. 10. In the first time window from -0.3 to 0.4 ps (Fig. 10a), in addition to the rising of the bands corresponding to the ^{1}BDP* and the $C_{60}^{\cdot-}$ as in the BDP-C_{60} dyad, TA spectra of the triad also show the appearance of weaker bands of ^{1}DSBDP* (ground state bleach (GSB) at 650 nm) due to the direct excitation of DSBDP at 525 nm ($\varepsilon_{(DSBDP,\ 525\ nm)}$ = 4000 $M^{-1}.cm^{-1}$). Since no ultrafast electron transfer (<1ps) from DSBDP to C_{60} was observed for the DSBDP-C_{60} dyad, the observation of $C_{60}^{\cdot-}$ reveals an ultrafast electron transfer from the Franck-Condon zone of ^{1}BDP* to C_{60}, similar to the BDP-C_{60} dyad.

In the second time window from 0.4 to 30 ps, a rapid recovery of BDP GSB with the concomitant increase of DSBDP GSB and the rise of ^{1}DSBDP* absorption bands at 455, 855 and 1000 nm are detected (Fig. 10b). These observations reveal the rapid excitation energy transfer from ^{1}BDP* to DSBDP. Then, ^{1}DSBDP* once formed follows the same sequence of photophysical events as observed in the DSBDP-C_{60} dyad. Briefly, the bands at 687 and 1045 nm corresponding to DSBDP$^{\cdot+}$ and $C_{60}^{\cdot-}$ continues to rise, due to electron transfer from ^{1}DSBDP* to C_{60} as observed in the DSBDP-C_{60} dyad. The charge-separated state (DSBDP$^{\cdot+}$-$C_{60}^{\cdot-}$) recombines in the third time-period from 30 to 300 ps (Fig. 10c) as evident by the decay of $C_{60}^{\cdot-}$ at 1045 nm and DSBDP$^{\cdot+}$ at 687 nm. Further, the absorption bands of ^{1}DSBDP* in the visible and NIR part decay due to the energy transfer process to C_{60} as already described for the DSBDP-C_{60} dyad. In the same time window, the recovery of the GSB of BDP suggests an energy transfer process to C_{60} consistent with the observations in the isolated BDP-C_{60} dyad.

Finally, in the fourth time panel above 300 ps, as in the DSBDP-C_{60} dyad, a second energy transfer in a more extended conformer causes a decay of ^{1}DSBDP* bands along with a recovery of GSB of DSBDP Finally, the TA spectra of last delay times show a formation of a mix of $^3C_{60}$* and ^{3}DSBDP* which was previously observed for the DSBDP-C_{60} dyad. In the triad also, the final excited state is ^{3}DSBDP* with the lifetime of (280 ± 20) μs, which was confirmed by nanosecond transient absorption measurements (SI Fig. 3b, green curve) [31].

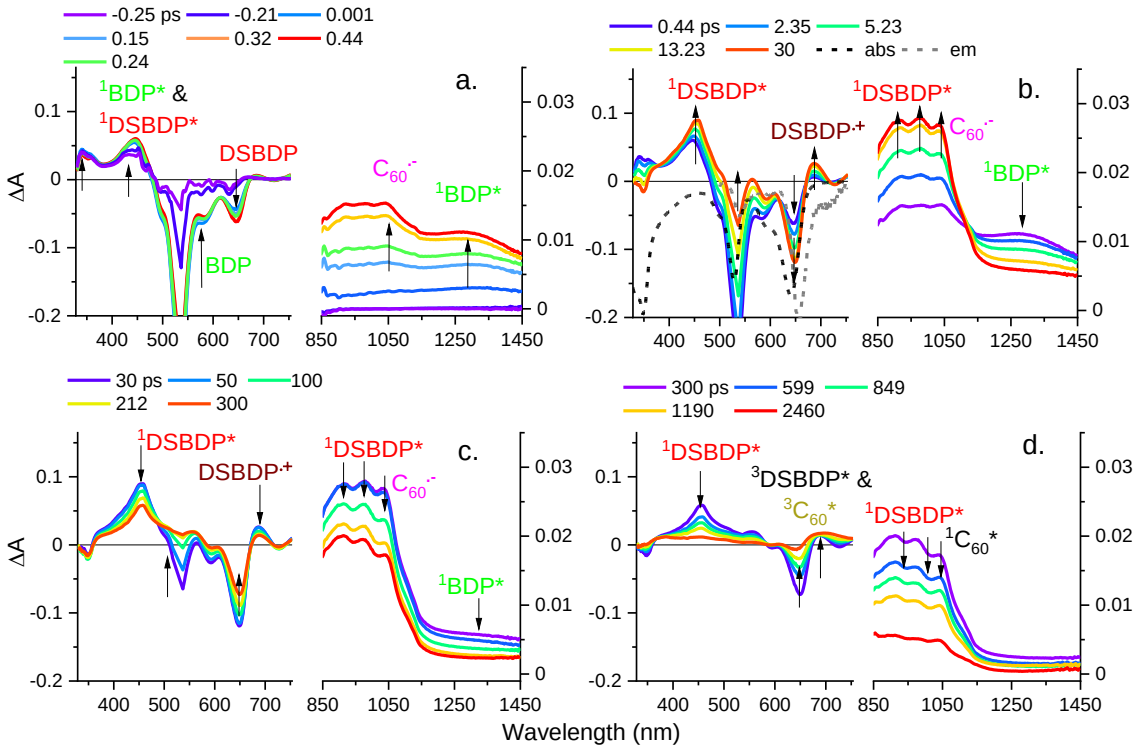

Fig. 10. Femtosecond transient absorption spectra of BDP-C_{60}-DSBDP at specified delay times: a) -0.25 to 0.44 ps; b) 0.44 to 30 ps; c) 30 to 300 ps and d) 300 to 2460 ps in solvent benzonitrile. λ_{exc} = 525 nm. The grey and black curves in panel b represent the respective ground state absorption (abs) and emission (em) spectra of the triad.

Kinetic analyses at specific wavelengths converged with a four-exponential model (SI Fig. 7). The analyses of the transient decays is sophisticated for the triad due to the overlap of different transient spectra (^{1}BDP*, ^{1}DSBDP*, BDP$^{\cdot+}$, DSBDP$^{\cdot+}$, $C_{60}^{\cdot-}$, $^1C_{60}$*, $^3C_{60}$* and ^{3}DSBDP*) and the occurring of simultaneous photophysical processes (electron/energy transfer) in similar timescales. The time constants obtained from the fit of several probe wavelengths corresponding principally to some transient species are detailed in SI Table 3. Moreover, the global fitting of kinetic traces converged with four time constants of <1 ps, 7, 68 and 595 ps. The DADS associated with the shortest time constant of <1 ps shows a rising component at the absorption of $C_{60}^{\cdot-}$, which is attributed to the ultrafast electron transfer from ^{1}BDP* to C_{60} in a short-distance conformer between BDP and C_{60}, as observed in BDP-C_{60} dyad. Moreover, an increase in DSBDP GSB at 650 nm is observed and can be assigned to an additional ultrafast energy transfer from ^{1}BDP* to DSBDP. This rising component is also obtained in the individual fit at the GSB band of DSBDP at 660 nm.

Further, the time constant of 7 ps could be related to two simultaneous processes. First, an additional increase in the DSBDP GSB band (positive band at 650 nm) is observed due to a second energy transfer from ^{1}BDP* to DSBDP, which was previously demonstrated in steady-state spectroscopy [31]. Second, a simultaneous rising of the $C_{60}^{\cdot-}$ band (negative band at 1045 nm) reveals an electron transfer from ^{1}DSBDP* to C_{60}.

Next, the DADS of 68 ps presents positive bands at 687 nm (DSBDP$^{\cdot+}$ absorption) and 1045 nm ($C_{60}^{\cdot-}$) which could be assigned to the decay of the charge-separated state (DSBDP$^{\cdot+}$-$C_{60}^{\cdot-}$). It should be noted that similar time constants for charge separation and recombination were obtained in the DSBDP-C_{60} dyad. Moreover, at the same time, the decay of BDP GSB at 525 nm is related to an energy transfer from ^{1}BDP* to C_{60} which is consistent with a time constant of about 50 ps obtained by individual fitting of the kinetic trace at 550 nm (BDP GSB). It should be reminded that 42 ps was obtained in the BDP-C_{60} dyad for the same process. This time component is also found in the fluorescence lifetime of ^{1}BDP* (Table 1) upon excitation at 495 nm. Also, the fluorescence decay of the triad shows a lifetime of 270 ps for DSBDP, which can be correlated to an energy transfer process from ^{1}DSBDP* to C_{60}. This component was also obtained in the individual fitting of the kinetic traces corresponding to the ^{1}DSBDP* (455 nm) and GSB DSBDP (660 nm) (SI Table 3), confirming the energy transfer process with a time constant of about 200 ps.

Subsequently, the last time constant of 595 ps is attributed to two simultaneous processes. A second energy transfer from ^{1}DSBDP* to C_{60} is evident by the decays of the ^{1}DSBDP* band at 455 nm and DSBDP GSB at 660 nm in the DADS. This time also agrees with the second fluorescence lifetime of DSBDP in the triad (880 ps, Table 1). The DADS also indicate the population of the triplet state of both $^3C_{60}$* and ^{3}DSBDP* at about 710 nm, revealing the ISC of $^1C_{60}$* and the ping-pong energy transfer between C_{60} and DSBDP as explained in the Section 3.4.2.

Fig. 12 summarizes all these photoinduced processes observed in the triad after excitation of BDP at 525 nm. The flexibility of the linkers leads to the presence of different families of conformers and consequently to multiple parallel processes. The accurate determination of the time constants for all these processes is impossible. The values shown in Fig. 12 are indicative and were obtained by the mean of different time-resolved techniques used in this study.

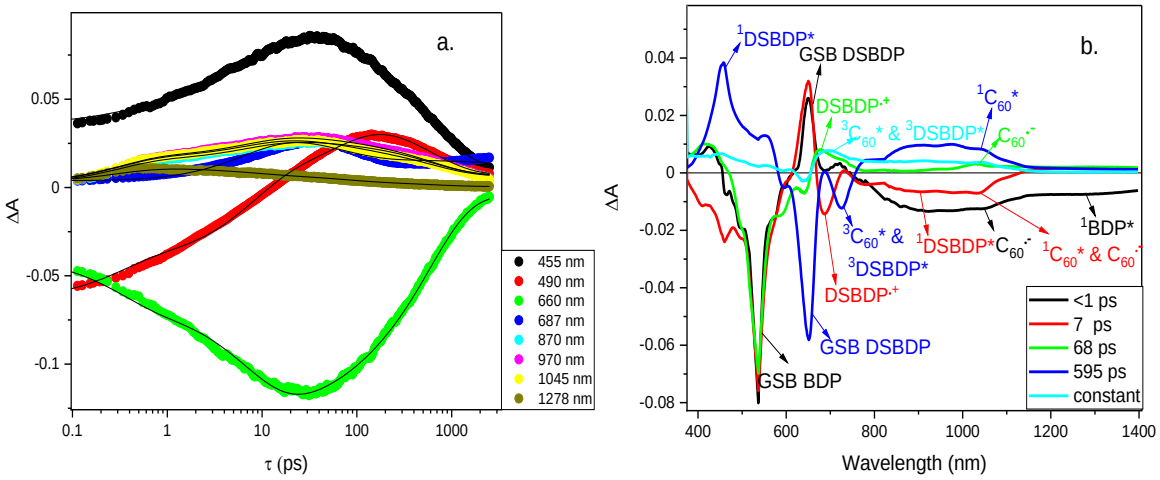

Fig. 11. a. Global fit of kinetic traces using a four exponential model and b. decay associated difference spectra (DADS) obtained by a global fit of femtosecond transient spectra of the BDP-C_{60}- DSBDP triad (λ_{exc} = 525 nm).

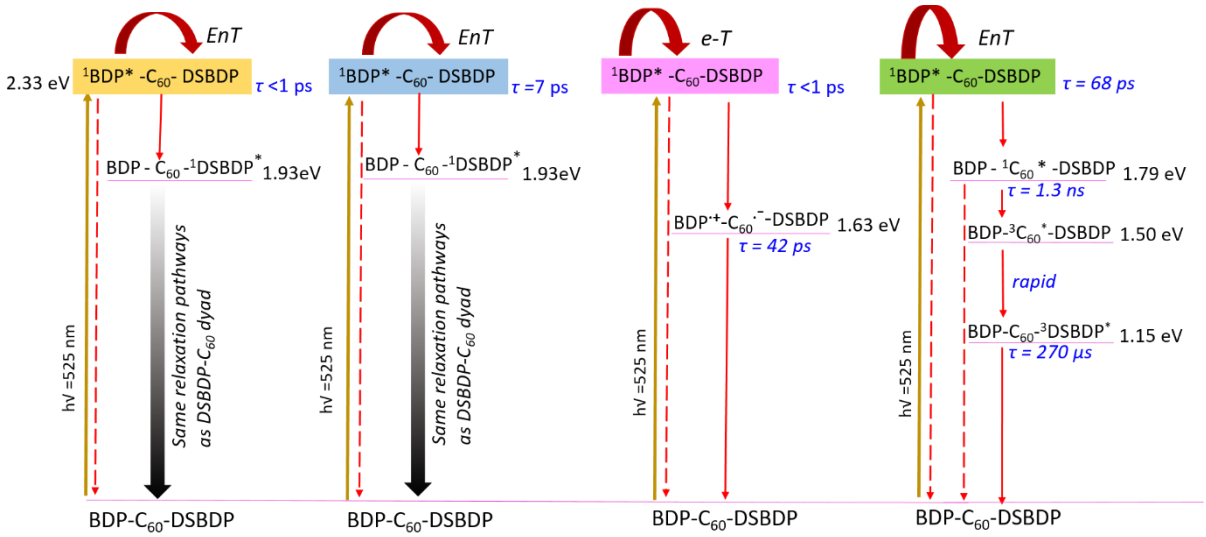

Fig. 12. Energy level diagram presenting the photoinduced processes in the BDP-C_{60}-DSBDP triad in argon saturated benzonitrile. ^{1}DSBDP* is formed by two energy transfer processes from ^{1}BDP* in <1 ps and 7 ps (two conformers). ^{1}BDP* also undergoes an ultrafast electron and an energy transfer process to C_{60}. ^{1}DSBDP* followed similar relaxation pathways as in the DSBDP-C_{60} dyad. The indicated lifetimes represent the kinetics of the dominant relaxation processes.

Further, femtosecond transient absorption measurements were also performed upon excitation of the DSBDP unit at 580 nm in the BDP-C_{60}-DSBDP triad. The femtosecond transient absorption spectra (SI Fig. 8) along with the individual and global fit are presented in SI Fig. 9 and SI Fig. 10, respectively. Almost identical spectral and kinetic features are observed as compared to those of the DSBDP-C_{60} dyad. This indicates similar relaxation pathways as that of the dyad when ^{1}DSBDP* is formed either by direct excitation or by an energy transfer from ^{1}BDP*.

Conclusion

We have elucidated the mechanistic details of complex photophysical processes within a broadband visible light-absorbing BDP-C_{60}-DSBDP triad together with the two reference BDP-C_{60} and DSBDP-C_{60} dyads. The photophysical characterization using ultrafast transient absorption and time-resolved emission methods revealed the presence of multiple conformations due to the flexible linker between the two BODIPY and C_{60} units. In the BDP-C_{60} dyad, an ultrafast electron transfer leads to the formation of a radical ion pair in a short BDP-C_{60} distance conformer. Additionally, two energy transfer processes from ^{1}BDP* to C_{60} were observed in two other conformers. In the DSBDP-C_{60} dyad, a rapid electron transfer and two energy transfer processes were also observed in conformers of different donor-acceptor distances. In the case of the triad, additional energy transfer processes from ^{1}BDP* to DSBDP were observed upon excitation of the BDP unit. Furthermore, ^{1}DSBDP* once formed followed the same relaxation pathways as that of the DSBDP-C_{60} dyad. The present triad in which the BODIPYs act as a light-harvesting antenna as well as electron donor contributes to the development of artificial molecular systems capable of mimicking photosynthetic "antenna-reaction center". For all these D-A systems with a flexible linker, a rapid photoinduced electron transfer from BODIPY to C_{60} was evidenced in conformers with close proximity of the D and A moieties, with a short lifetime of the charge-separated state. This will be taken into account for the design of the next generations of BODIPY based D-A systems. Works are under progress in our laboratory to improve the lifetime of the charge-separated state by adding supplementary electron donor as ferrocene. With the scarce reporting on the ultrafast processes in covalently-linked flexible systems, the intriguing photophysics of this broadband energy harvesting triad will provide useful fundamental insights for the development of covalently linked donor-acceptor assemblies for solar energy applications.

Supplementary Information
The online version contains available supplementary material.

Acknowledgements
This work was supported by the CNRS (International Emerging Action, PICS project n° 08198), the LabEx PALM ANR-10LABX-0039-PALM and CHARMMMAT ANR-11-LABX-0039, Région Ile-de-France DIM Nano-K. Anam Fatima is grateful for the MESRI grant (2019-2022). Jad Rabah thanks the MESRI for a PhD fellowship (2017-2020).

Statements and Declarations
On behalf of all authors, the corresponding authors state that there is no conflict of interest.

References

[1] V. Balzani, A. Credi & M. Venturi, *ChemSusChem* **1**, 26–58 (2008).
[2] D. Gust, T. A. Moore & A. L. Moore, *Acc. Chem. Res.* **42**, 1890–1898 (2009).
[3] F. D'Souza & O. Ito, *Chem. Comm.* 4913–4928 (2009).
[4] D. M. Guldi, B. M. Illescas, C. M. Atienza, M. Wielopolski & N. M. Martı´n, *Chem. Soc. Rev.* **38,** 1587-1597 (2009)
[5] M. E. El-Khouly, S. Fukuzumi, & F. D'Souza, *ChemPhysChem* **15**, 30–47 (2014).
[6] F. D'Souza & O. Ito, *Coord. Chem. Rev.* **249**, 1410–1422 (2005).
[7] G. Kodis, Y. Terazono, Liddell, A. Paul, J.Andre, V. Garg, M. Hambourger, T. A. Moore, A. L. Moore & D. Gust, *J. Am. Chem. Soc.* **128,** 1818–1827 (2006).
[8] C. Luo, D. M. Guldi, H. Imahori, K. Tamaki, & Y. Sakata, *J. Am. Chem. Soc.* **122**, 6535–6551 (2000).
[9] F.D'Souza, P. Smith, M. Zandler, A. McCarty, M. Itou, Y. Araki & *O. Ito, J. Am. Chem. Soc.* **126**, 7898–7907 (2004).
[10] T. Lazarides, G. Charalambidis, A. Vuillamy, M. Réglier, E. Klontzas, G. Froudakis, S. Kuhri, D. M. Guldi & A. Coutsolelos, *Inorg. Chem.* **50**, 8926–8936 (2011)
[11] M. E. El-Khouly, C. A. Wijesinghe, V. N. Nesterov, M. E. Zandler, S. Fukuzumi & F. D'Souza, *Chem. - A Eur. J.* **18**, 13844–13853 (2012).
[12] Y. Rio, S. Wolfgang, A. Gouloumis, P. Vázquez, J. L. Sessler, D. M. Guldi & T. Tomás, *Chem. - A Eur. J.* **16**, 1929–1940 (2010).
[13] A. Loudet & K. Burgess, *Chem. Rev.* **107**, 4891–4932 (2007).
[14] G. Ulrich, R. Ziessel, & A. Harriman, *Angew. Chem. Int. Ed. Engl.* **47**, 1184–1201 (2008).
[15] C. O. Obondi, G. N. Lim P. A. Karr, V. N. Nesterov & F. D'Souza, *Phys. Chem. Chem. Phys.* **18**, 18187–18200 (2016).
[16] J. Y. Liu, H. S. Yeung, W. Xu, X. Li & D. K. P. Ng, *Org. Lett.* **10**, 5421–5424 (2008).
[17] M. Rudolf, S. V. Kirner & D. M. Guldi, *Chem. Soc. Rev.* **45**, 612–630 (2016).
[18] D. M. Guldi & M. Prato, *Acc. Chem. Res.* **33**, 695–703 (2000).
[19] A. N. Amin, M. El-Khouly, N. Subbaiyan, M. E. Zandler & S. Fukuzumi, *Chem. Commun.* **48**, 206–208

(2012).
[20] A. Iagatti, L. Cupellini, G. Biagiotti, S. Caprasecca, S. Fedeli, A. Lapini, E. Ussano, S. Cicchi, P. Foggi, M. Marcaccio, B. Mennucci & M. Di Donato, *J. Phys. Chem. C* **120**, 16526–16536 (2016).
[21] J. Y. Liu, M. E. El-Khouly S. Fukuzumi, & D. K. Ng, *Chem. – An Asian J.* **6**, 174–179 (2011).
[22] C. A. Wijesinghe, M. El-Khouly, J. Blakemore, M. Zandler, S. Fukuzumi & F. D'Souza, *Chem. Commun.* **46**, 3301 (2010).
[23] V. Bandi, H. B. Gobeze, & F. D'Souza, *Chem. - A Eur. J.* **21**, 11483–11494 (2015).
[24] T.-T. Tran, J. Rabah, M. H. Ha-Thi, E. Allard, S. Nizinski, G. Burdzinski, S. Aloïse, H. Fensterbank, K. Baczko, H. Nasrallah, A. Valée, G. Clavier, F. Miomandre, T. Pino & R. Méallet-Renault, *J. Phys. Chem. B* **124**, 9396–9410 (2020).
[25] V. Bandi, F. P. D'Souza, , H. B. Gobeze & F. D'Souza, *Chem. Commun.* **52**, 579–581 (2015).
[26] C. O. Obondi, G. N. Lim, P. Martinez, V. Swamy & F. D'Souza, *Nanoscale* **9**, 18054–18065 (2017).
[27] N. Zarrabi, C. O. Obondi, G. N. Lim, S. Seetharaman, B. J. Boe, F. D'Souza & P. K. Poddutoori, *Nanoscale* **10**, 20723–20739 (2018).
[28] S. Shao, M. B. Thomas, K. H. Park, Z. Mahaffey, D. Kim & F. D'Souza, *Chem. Commun.* **54**, 54–57 (2018).
[29] V. Bandi, F. P. D'Souza, H. B. Gobeze & F. D'Souza, *Chem. - A Eur. J.* **21**, 2669–2679 (2015).
[30] J. Rabah, L. Yonkeu, K. Wright, A. Vallée, R. Méallet-Renault, M. H. Ha-Thi, A. Fatima, G. Clavier, H. Fensterbank & E. Allard, *Tetrahedron* 132467 (2021).
[31] A. Fatima, J. Rabah, E. Allard, H. Fensterbank, K. Wright, G. Burdzinski, G. Clavier, M. Sliwa, T. Pino, R. Méallet-Renault, K. Steenkeste & M. H. Ha-Thi, Selective Population of Triplet Excited States in Heavy Atom Free BODIPY-C_{60}-DSBDP Based Molecular Assemblies, *Photochem. Photobiol. Sci.* accepted (2022).
[32] A. Ghose, M. Rebarz, O. Maltsev, L. Hintermann, C. Ruckebusch, E. Fron, J. Hofkens, Y. Mély, P. Naumov, M. Sliwa & P. Didier, *J. Phys. Chem. B* **119**, 2638–2649 (2015).
[33] M. Wendel, S. Nizinski, D. Tuwalska, K. Starzak, D. Szot, D. Prukala, M. Sikorski, S. Wybraniec & G. Burdzinski, *Phys. Chem. Chem. Phys.* **17**, 18152–18158 (2015).
[34] T. Chaudhuri, S. Mula, S. Chattopadhyay & M. Banerjee, *Spectrochim. Acta Part A Mol. Biomol. Spectrosc.* **75**, 739–744 (2010).
[35] T. D. M. Bell , K. P. Ghiggino, A. Haynes, S. J. Langford & C. P. Woodward, *J. Porphyr. Phthalocyanines* **11**, 455–462 (2007).
[36] V. Bandi, H. B. Gobeze, V. Lakshmi, M. Ravikanth & F. D'Souza, *J. Phys. Chem. C* **119**, 8095–8102 (2015).
[37] L. Huang, X. Yu, W. Wu & J. Zhao, *Org. Lett.* **14**, 2594–2597 (2012).